Title
ON FLUID RESERVES AND THE PRODUCTION OF SUPERHEATED STEAM FROM FRACTURED, VAPOR-DOMINATED GEOTHERMAL RESERVOIRS

Permalink
https://escholarship.org/uc/item/80z1c2s5

Authors
Pruess, K.
Narasimhan, T.N.

Publication Date
1981-07-01

Lawrence Berkeley Laboratory
UNIVERSITY OF CALIFORNIA, BERKELEY

EARTH SCIENCES DIVISION

Submitted to the Journal of Economic Geology

ON FLUID RESERVES AND THE PRODUCTION OF SUPERHEATED STEAM FROM FRACTURED, VAPOR-DOMINATED GEOTHERMAL RESERVOIRS

K. Pruess and T.N. Narasimhan

July 1981

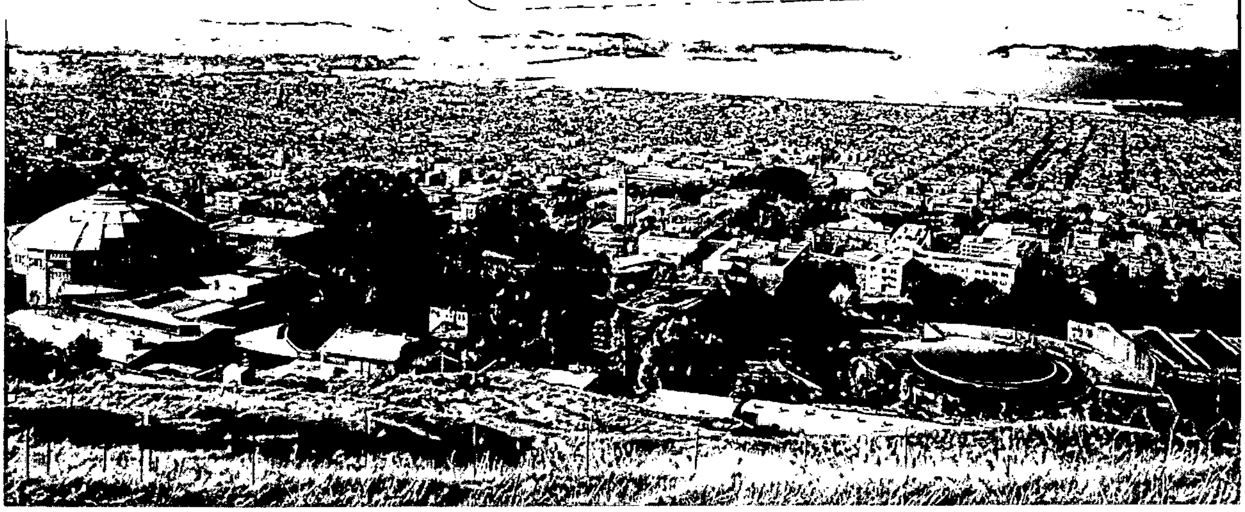

Prepared for the U.S. Department of Energy under Contract W-7405-ENG-48

ON FLUID RESERVES AND THE PRODUCTION OF SUPERHEATED STEAM FROM FRACTURED, VAPOR-DOMINATED GEOTHERMAL RESERVOIRS

K. Pruess and T.N. Narasimhan
Earth Sciences Division
Lawrence Berkeley Laboratory
University of California
Berkeley, CA 94720

Abstract

Vapor-dominated geothermal reservoirs produce saturated or superheated steam, and vertical pressure gradients are close to vapor-static. These observations have been generally accepted as providing conclusive evidence that the liquid saturation must be rather small ($<$ 50%) in order that liquid may be nearly immobile. This conclusion ignores the crucial role of conductive heat transfer mechanisms in fractured reservoirs for vaporizing liquid flowing under two-phase conditions. We have developed a multiple interacting continuum method (MINC) for numerically simulating two-phase flow of a homogeneous fluid in a fractured porous medium. Application of this method to reservoir conditions representative of The Geysers, California, and results from an analytical approximation show that, for matrix permeability less than a critical value ($\approx$ 2.5 to 5 microDarcies), the mass flux of water from the matrix to the fractures will be continuously vaporized by heat transported due to conduction. This gives rise to production of superheated steam even when the matrix has nearly full liquid saturation.

Simple estimates also show that heat-driven steam/water counterflow can maintain a nearly vapor-static vertical pressure profile in the presence of mobile liquid water in a reservoir with low vertical matrix permeability. The implication of these findings is that the fluid reserves of vapor-dominated geothermal reservoirs may be larger by a factor of about two than has generally been believed in the past.

1. Introduction

Only a few geothermal reservoirs are known worldwide which produce saturated or slightly superheated steam, typically at temperatures near 240 °C (e.g, Larderello, Italy; The Geysers, California; Matsukawa, Japan; Kawah Kamojang, Indonesia). Even though liquid-dominated reservoirs are much more numerous, the vapor-dominated systems are more easily exploited and currently provide the main source of geothermal electric power. After much controversy in the earlier literature (summarized e.g. by Truesdell and White, 1973), a consensus was reached that most of the mass reserves in a vapor-dominated geothermal reservoir are in place in liquid form (Marconcini et al., 1977). This is usually concluded on the basis of total cumulative production in fields like Larderello, Italy, or The Geysers, California, which would require unreasonably large reservoir thickness if the fluids are assumed to be stored in the form of steam (James, 1968; Nathenson, 1975; Weres et al., 1977).

There is still considerable uncertainty as to where exactly the liquid water resides, and how much liquid is present in the reservoir (Weres et al., 1977; Celati et al., 1979). Virtually all wells in Larderello and at The Geysers produce saturated or slightly superheated steam, with no direct evidence for the presence of liquid water in the reservoir. White, Muffler, and Truesdell (1971) have proposed a general conceptual model of vapor-dominated reservoirs which postulates the existence of liquid water dispersed throughout the reservoir, as well as a deep water table, presumably containing rather saline brine. While there is some indication that deep wells may have penetrated a zone approaching hydrostatic pressure gradients in Larderello, there is no evidence for a deep water table at The Geysers in the published literature. Further elaborating on their model, Truesdell and White (1973) have presented convincing evidence for the existence of dispersed water, noting that early (pre-exploitation) records of temperature and pressure are always close to saturated conditions, thus indicating the presence of a two-phase steam/water mixture. Failure to observe the liquid water is attributed to in-place vaporization as a consequence of production-induced pressure decline. From a consideration of production enthalpies, Truesdell and White suggest that the saturation (pore volume fraction) of liquid water in the natural, undisturbed state of the Larderello reservoir is in the range of 20% to at most 50%. Similar estimates have been made for The Geysers reservoir (Dykstra, 1981). Significantly higher water saturations are excluded, because reservoir pressures are controlled by steam (vapor-static). It is generally accepted that the residual immobile saturation for liquid water is in the range of 30% - 50%, and this is considered an upper limit for the dispersed water saturation in a vapor-dominated reservoir. If water saturation were to significantly exceed this value, water would become mobile and would presumably tend to establish a hydrostatic rather than a vapor-static pressure gradient. However, there appears to be a general agreement that liquid water is somewhat mobile, providing for a steam/water counter flow mechanism which is a very effective means of transporting heat upwards under conditions of small vertical temperature gradients (Eastman, 1968).

We find it difficult to accept water saturations as low as 30% to 50% for the natural state of a vapor-dominated reservoir, except in certain regions as e.g. near natural vents. Simulation studies using a realistic numerical model of a vapor-dominated reservoir have shown that water saturations are generally large, and that the system tends to remain water saturated at depth and near the margins (Pruess and Truesdell, 1980). This is consistent with geochemical evidence for vaporization and condensation processes in Larderello and at The Geysers (D'Amore and Truesdell, 1979). If one were to accept a mobile liquid phase in vapor-dominated reservoirs, how could this be reconciled with nearly vapor-static pressure gradients and the fact that wells completed near reservoir margins or at great depth nonetheless tend to produce superheated steam, sometimes after an initial wet discharge? It is the purpose of this paper to suggest that these seemingly contradictory attributes can occur simultaneously in fractured porous reservoirs with low matrix permeability. Significantly, all known vapor-dominated reservoirs are of this type. We shall show that the physical characteristics of these systems and their response to production are very substantially altered by heat conduction in the matrix. The arguments limiting water saturation to nearly immobile levels based on a consideration of pressure gradients, and the model of Truesdell and White, ignore the crucial effect of heat conduction on flowing two-phase mixtures. Conventional wisdom has held that heat conduction is a process too slow to have significant impact on the response of geothermal reservoirs to production. This consideration is certainly valid for porous-media type reservoirs with permeabilities large enough to be of practical interest. However, in fractured two-phase reservoirs with low matrix permeability, heat conduction can strongly increase the flowing enthalpy and it is actually possible to produce superheated steam from a rock matrix with liquid saturation approaching 100%. Also, water saturations approaching 100% can be compatible with an essentially vapor-static pressure gradient with depth. These conclusions, to be detailed below, suggest that total fluid reservers of vapor-dominated geothermal reservoirs may be significantly larger than was believed previously.

2. The Concept of Limiting Effective Permeability

Consider a two-phase mixture of water and steam flowing in a homogeneous porous medium. Ignoring gravity effects for the moment, the mass flux for phase α can be written (please see "Notation" for explanation of symbols):

$$\underset{\sim}{F}_\alpha = - k \frac{k_\alpha}{\mu_\alpha} \rho_\alpha \nabla P \qquad (1)$$

Variations in pressure and temperature are related by the Clapeyron equation:

$$\frac{dT}{dP} = \frac{(v_v - v_\ell)(T + 273.15)}{(h_v - h_\ell)} \qquad (2)$$

Therefore, there is a one-to-one correspondence between mass flux and the conductive heat flux given by:

$$\underset{\sim}{q} = - K \nabla T \qquad (3)$$

The conductive heat flux effectively gives rise to an increase in flowing enthalpy of the two-phase mixture, causing part or all of the liquid to vaporize and possibly to acquire superheat. The fraction of liquid flux vaporized is:

$$\nu_o = \frac{|\underset{\sim}{q}|}{|\underset{\sim}{F}_\ell| \, (h_v - h_\ell)} = \frac{k_{lim}(K,T)}{k k_\ell} \qquad (4)$$

where we have defined a limiting effective permeability, dependent upon heat conductivity and temperature, as:

$$k_{lim}(K,T) = K \frac{\mu_\ell v_\ell (v_v - v_\ell)(T + 273.15)}{(h_v - h_\ell)^2} \qquad (5)$$

k_{lim} is plotted as a function of temperature in Figure 1. For typical conditions in vapor-dominated geothermal reservoirs, T = 240 °C and 2 W/m°C $\leq$ K $\leq$ 4 W/m°C, the limiting effective permeability is seen to be of the order of 2.5 - 5.0 x 10^{-18} m^2 ($\cong$ 2.5 - 5.0 microDarcies).

Under conditions where gravity effects are negligible (large pressure gradients or small vertical permeability) the significance of k_{lim} is as follows. If the effective permeability $k \cdot k_\ell$ for the liquid phase is equal to or less than k_{lim} (i.e., $\nu_o \geq 1$), it is impossible to draw liquid water out of a porous medium containing a two-phase steam/water mixture. Rather, liquid is completely vaporized as it flows, with heat of vaporization provided by conduction. Note that vaporization can also occur due to heat transfer from "local" rock in contact with liquid. Even if liquid saturation approaches 100% (and therefore $k_\ell \rightarrow 1$), withdrawal of fluid from a porous medium with $k < k_{lim}$ will result in the production of superheated steam, irrespective of whether the applied flow rate is large or small. In order to extend this analysis to gravity effects, we decompose the pressure gradient into horizontal and vertical components, $\nabla p = \frac{\partial p}{\partial r} \underset{\sim}{e}_r + \frac{\partial p}{\partial z} \underset{\sim}{e}_z$. A straightforward calculation shows that the fraction of liquid flux vaporized can be written as:

$$\nu = \nu_o \cdot \nu_g = \frac{k_{lim}(K,T)}{kk_\ell} \nu_g \qquad (6)$$

where the additional factor introduced by gravity is

$$\nu_g = \frac{\left(\frac{\partial p}{\partial r}\right)^2 + \frac{k_z}{k}\left[\frac{\partial p}{\partial z} + \rho_\ell g\right]\frac{\partial p}{\partial z}}{\left(\frac{\partial p}{\partial r}\right)^2 + \left(\frac{k_z}{k}\right)^2\left[\frac{\partial p}{\partial z} + \rho_\ell g\right]^2} \qquad (7)$$

It is seen that gravity effects will be small ($\nu_g \rightarrow 1$) if pressure gradients are large, or if vertical permeability is small compared to horizontal permeability. Conductive vaporization will vanish ($\nu_g = 0$) in the absence of pressure gradients, as it must, when liquid flows only by gravitational force. If horizontal pressure gradients are small, ν_g can become negative for vertical pressure gradients less than hydrostatic, indicating that heat conduction diminishes the enthalpy of flowing liquid (liquid flows downward while heat conduction is upward). This is the situation typically encountered in the natural state of the central portion of vapor-dominated geothermal reservoirs. However, larger-than-hydrostatic vertical pressure gradients can result in large positive ν_g.

To further elucidate the significance of the limiting effective permeability let us again consider the "no gravity" case, applicable to situations with predominantly horizontal pressure gradients (flow to a well) and for small vertical permeability. Given a certain functional dependence of relative permeability upon liquid saturation, $k_\ell = k_\ell(S_\ell)$, it is possible to determine, as a function of absolute permeability k, the saturation S_ℓ at which the effective permeability kk_ℓ will drop below the limiting effective permeability k_{lim}, thus resulting in 100% vaporization of flowing liquid:

$$k_\ell(S_\ell) = \frac{k_{lim}(K,T)}{k} \qquad (8)$$

At typical conditions of K = 4 W/m°C, T = 240 °C, we have $k_{lim} = 5.27 \times 10^{-18}\ m^2$. In Figure 2 we have plotted S_ℓ as a function of k, from eq. (8), for Corey-type relative permeability functions with residual immobile water saturation $S_{\ell r}$ in the range from 10% to 50% (Faust and Mercer, 1979).

$$k_\ell = S^{*4} \qquad (9a)$$

$$k_v = (1-S^*)^2(1-S^{*2}) \qquad (9b)$$

where

$$S^* = \frac{S_\ell - S_{\ell r}}{1 - S_{\ell r} - S_{sr}} \qquad (9c)$$

It is seen that even at permeabilities as large as 10^{-15} m^2 (approximately 1 milliDarcy) water saturations some 10% in excess of residual immobile saturation will result in production of superheated steam. These general conclusions have been confirmed by means of numerical simulations, to be discussed below.

3. Vertical Pressure Gradients and Steam/Water Counterflow

Let us now consider the question whether large water saturations ($S_\ell \rightarrow 1$) and a highly mobile liquid phase ($k_\ell \rightarrow 1$) can be compatible with the observed vertical pressure gradients in vapor-dominated reservoirs. In the central portion of a vapor-dominated reservoir, these gradients are much smaller than hydrostatic, and are actually close to vapor-static (White et al., 1971). Therefore, mobile water will drain downward. The drainage occurs in the direction of the (small) vertical pressure and temperature gradient, so that heat conduction actually diminishes the flowing enthalpy. Thus the mechanism discussed in Section 2 is not operative, and liquid water may drain gravitationally from low-permeability rocks without being flashed into steam. The downflow of liquid will tend to establish a hydrostatic pressure gradient with depth, unless it is balanced by an upflow of steam such that the net vertical mass transport vanishes. A balanced (no net mass transport) steam/water counterflow is possible if two conditions are met: (i) gravitational drainage must be inhibited by small vertical permeability for the liquid phase, while vertical permeability must be much larger for the vapor phase; and (ii) the magmatic heat source must be powerful enough to generate the large heat fluxes necessary to drive a balanced steam/water counterflow system.

It has long been recognized in the literature that capillary forces will tend to hold liquid water in smaller pores (Truesdell and White, 1973), whereas vapor will occupy the larger pores and fractures. The discussion of Section 2 suggests why liquid cannot be present in the vertical fractures: in order to enter vertical fractures from the low-permeability rock matrix, liquid flow has to have a horizontal (pressure driven) component, and is then subject to flashing by conduction. Therefore, gravitational drainage is governed by the small vertical matrix permeability, while vertical upflow of steam has the much larger permeability in the fractures available. Thus, it is not necessary to invoke relative permeability effects and a nearly immobile liquid water saturation to explain why vertical permeability for vapor will be much larger than that for liquid (condition (i), above) in reservoirs with predominantly vertical fracture orientation, such as The Geysers (Lipman et al., 1977).

In order to assess whether typical vertical heat fluxes of vapor-dominated systems are sufficient to maintain steam/water counterflow for a highly mobile liquid phase (S_ℓ, $k_\ell \rightarrow 1$), we need to quantitatively examine the applicable permeability constraints. The condition for "balanced" (no net mass transport) steam/water counterflow is:

$$\underset{\sim}{F}_v = - \underset{\sim}{F}_\ell \qquad (10)$$

From Darcy's law including gravity effects (replace ∇p with $\nabla p - \rho_\alpha \underset{\sim}{g}$ in eq.(1)) we obtain a relationship between vertical pressure gradient dp/dz and the ratio of vertical permeabilities for liquid and vapor:

$$\frac{k_1 k_\ell}{k_2 k_v} = - \frac{\rho_v \mu_\ell (dp/dz + \rho_v g)}{\mu_v \rho_\ell (\rho_\ell g + dp/dz)} \quad (11)$$

The upward convective heat flux is:

$$q = - \frac{k_2 k_v}{\mu_v} (h_v - h_\ell) \rho_v (dp/dz + \rho_v g) \quad (12)$$

Data published by Ramey (1968) indicate that the vertical heat flux near the surface can be as large as 4 W/m^2 in some areas of The Geysers. Assuming a value of $q = 4$ W/m^2 for the convective heat flux resulting from steam/water counterflow, we use eq. (12) to compute the required vertical permeability $k_2 k_v$ for vapor as a function of vertical pressure gradient dp/dz. In Figure 3 we have plotted $k_2 k_v$ for T = 240 ^{o}C against the "excess" vertical pressure gradient γ, expressed in units of the vapor-static gradient $- \rho_v g$ $\left(\gamma = - \frac{dp/dz}{\rho_v g} - 1\right)$. From eq. (12) it is obvious that this plot results in a straight line on log-log paper. For a realistic vertical pressure gradient of twice the vapor-static value, we require a vertical permeability of 14.4 x 10^{-15} m^2 ($\cong$ 14 milliDarcy) for steam, which is an entirely plausible value for the average vertical fracture permeability at The Geysers. We have also plotted the vertical permeability $k_1 k_\ell$ for liquid from eq. (11). This is nearly independent of pressure gradient as long as the gradient (absolute value) is much smaller than the hydrostatic value $\rho_\ell g$. The vertical liquid permeability is 40 x 10^{-18} m^2 ($\cong$ 40 microDarcies), which appears to be a plausible value for vertical matrix permeability at The Geysers. If vertical matrix permeability is larger, a balanced steam/water counterflow requires a somewhat smaller liquid saturation, $S_\ell < 1$, so that $k_1 k_\ell (S_\ell) = 40 \times 10^{-18}$ m^2. If $k_1 k_\ell$ is less than this value, a net upward mass transport will result (steam upflow exceeding water downflow). Such a condition is expected to prevail in the central portion of vapor-dominated reservoirs. From eq. (12) it is seen that the permeabilities as plotted in Figure 3 depend linearly upon the assumed heat flux (here $q = 4$ W/m^2). Thus it is straightforward to extend this analysis to different values of heat flux and vertical pressure gradients. It is interesting to note that the limit for vertical liquid permeability from a consideration of balanced steam/water counterflow is significantly larger than the limiting effective permeability discussed in Section 2. We conclude that the requirement that only steam be produced from a fractured two-phase reservoir with mobile liquid phase actually places more stringent limits on matrix permeability and liquid saturation than the requirement of a balanced steam/water counterflow.

4. A Multiple Interacting Continuum Method for Fractured Porous Media

We have developed a "multiple interacting continuum" technique (MINC) for numerically simulating heat and fluid flow in fractured porous media. A detailed discussion of this method, which is generally applicable to transient multi-component, multi-phase thermal processes, is given in Pruess and Narasimhan (1981). Here we shall briefly review the basic features of the MINC-method.

For simplicity we shall consider an idealized fractured reservoir, made up of identical rectangular blocks which are separated by fractures (Figure 4). This reservoir model is similar to the one employed by Warren and Root in their well-known double-porosity model (Warren and Root, 1963). However, Warren and Root make several simplifying approximations, such as restriction to one-component isothermal flow, and quasi-steady flow between blocks and fractures, in order to obtain an analytically solvable problem. In contrast, we have been able to relax many of the Warren and Root assumptions since we have taken a more general numerical approach. Thus, our numerical method treats transient fluid and heat flow within the blocks, between blocks and fractures, and in the fractures.

The main difficulty in modeling thermal processes in a fractured medium is that strong variations in thermodynamic conditions between fractures and blocks occur over small distances. For example, in a producing vapor-dominated geothermal reservoir one may encounter superheated steam in fractures, whereas a short distance away there may be plenty of pore water in the blocks. Boiling of this water will create large temperature gradients which may persist over long periods of time, since conductive thermal equilibration is a slow process.

For purposes of numerical simulation, it is necessary to subdivide a flow domain into volume elements, or grid blocks, within each of which there must be approximate thermodynamic equilibrium at all times. Only if this condition is met is it possible to associate average temperatures and pressures with each grid block, and to express interblock (fluid and heat) flows in terms of these averages. In order to obtain a suitable computational mesh for a fractured porous medium, it is important to note that variations in thermodynamic conditions will be much less pronounced in the direction of a fracture than perpendicular to it. It is therefore a good first approximation to assume that thermodynamic conditions will depend only upon the distance from the nearest fracture. Therefore, we shall subdivide the flow domain into computational volume elements in such a way that all interfaces between volume elements are parallel to the nearest fracture. This gives rise to a pattern of nested volume elements as shown in Figure 5, with each element having a definite thermodynamic state assigned to it. Numerical simulation of fluid and heat flow in such a system of nested volume elements, or interacting continua, is most conveniently made within the framework of an integral finite difference formulation (IFD) (Narasimhan, 1980). The required geometrical information--element volumes, interface areas, and nodal distances--is generated by a pre-processor program from a specification of widths, orientations, and spacings of fracture sets. While the calculations presented below employ a regular fracture network for convenience (Figures 4 and 5), the method can be generalized to arbitrary assemblages of fractures which may be described in a statistical fashion.

We shall now introduce a generalization, within the context of a regular fracture network, which considerably enhances scope and applicability of the concepts discussed above. In reservoir regions where spatial variations are small, it is not necessary to have separate volume elements within each of the elementary units depicted in Figure 5. Instead, corresponding nested volumes in neighboring units, which are identified by an index number in Figure 5, can be lumped together into one computational volume element. Element volumes and interface areas scale proportional to the number of elementary units which are lumped together, whereas nodal distances remain unchanged. The scaling can be further generalized to grid blocks of arbitrary shape and size. Thus we arrive at a two-step procedure for defining a computational mesh for a fractured reservoir. The first step is to construct a mesh just as would be done for a porous-medium type system, with small grid blocks near wells, etc. The second step is to sub-partition each grid block into several continua, the respective volumes, interface areas, and nodal distances of which are obtained by appropriate scaling from the quantities pertaining to the basic fractured unit.

Properly speaking, in regions where small grid blocks are desirable for spatial resolution, e.g. near wells, one should attempt to model individual fractures. A description based on average fracture spacings is appropriate in the more distant portions of the reservoir, where less detail is available and desirable. However, we believe it useful to be able to extend a fracture description based on average parameters (spacings, widths, orientations) to small volume elements, because this is applicable in cases where no detailed information about individual fractures near a well is available.

5. Simulation of Production from a Fractured Two-Phase Reservoir

We have implemented the MINC-method as discussed above in conjunction with our two-phase, non-isothermal geothermal reservoir simulator SHAFT79 (Pruess and Schroeder, 1980). The method was validated by comparison with the model of Warren and Root, which is contained within the general MINC framework as a special case. Subsequently, several simulations of two-phase flow to a well penetrating a fractured reservoir were carried out.

Previous application of numerical simulation techniques to fractured geothermal reservoirs were reported by Moench and coworkers (1978, 1979, 1980). These authors consider a one-dimensional set of plane horizontal fractures separated by blocks of low permeability and porosity. The system is modeled by straightforward subdivision of the flow region into simply connected volume elements. The rock matrix can interact with the fractures by means of heat conduction and steam flow. Liquid water is assumed to be immobile throughout, even at saturations as high as $S_\ell = 80\%$. The fractures are treated as extended regions of high permeability, with a typical thickness of .2 to 1.0 m.

We have attempted to model the interaction between reservoir matrix and fractures in a more realistic way, with conceptual model and parameters chosen to be applicable to steam wells at The Geysers reservoir. This field has excellent horizontal permeability, but core analysis seems to indicate that most fractures are nearly vertical (Lipman et al., 1977). We have idealized this situation by introducing three orthogonal sets of equidistant fractures as indicated in Figure 4. Modeling of such a system with the conventional simply connected volume elements would require a prohibitively large number of grid blocks, and therefore the MINC-method with nested volume elements is used. Also, we allow for liquid water to be mobile in the matrix and in the fractures.

Counsil and Ramey (1979) have carried out relative permeability experiments from which they obtain a residual immobile liquid saturation as large as $S_{\ell r} = .7$. However, their method of analysis (Arihara, 1974) appears to neglect the enhancement of effective flowing enthalpy due to heat conduction, as discussed in section 2. This approximation would tend to underestimate liquid flow, and therefore give too large values for $S_{\ell r}$. We consider Counsil and Ramey's value of $S_{\ell r} \approx .4$ as determined from an isothermal gas-water flow experiment more realistic. In the simulations we use Corey-type relative permeability curves (eqs. 9a-c) with $S_{\ell r} = .3$, $S_{sr} = .05$. Published reservoir data for The Geysers are not plentiful, but the information given by Ramey (1968), Lipman et al., (1977), and Dykstra (1981) is sufficient to define a representative case. The parameters used in the calculations are summarized in Table 1. We are mainly interested in comparing production enthalpies for fractured and porous medium-type conditions in the presence of mobile water. Enthalpy transients and the occurrence of superheated steam depend strongly on flow rates and pressure gradients in the vicinity of the well, so that it is important to have a realistic description of effective wellbore radius (skin). All commercial wells at The Geysers intersect one or several major fractures, giving rise to negative skin values and large effective wellbore radii. We have adopted parameters similar to those obtained by Koenig and Sanyal (1981) from pressure transient tests for two typical Geysers wells. We include a realistic storage volume for the wellbore, in order to avoid early time transients resulting from the mathematical artifact of a step rate change in flow at the sandface.

Fracture spacing was chosen to be D = 50 m in all calculations, which we believe to be representative of conditions at The Geysers, based on typical numbers of steam entries in wells (Dykstra, 1981). Fracture width δ is then determined from the total required permeability-thickness product according to:

$$kh = 2 \frac{h}{D} k_f \delta \tag{13}$$

The factor 2 appears because, due to the presence of three orthogonal fracture sets, there are two fracture sets available for flow in any given direction. The permeability of an individual fracture is related to its width by the well known relation (Witherspoon et al., 1980):

$$k_f = \delta^2/12 \tag{14}$$

In constrast to Moench et al. (1978, 1979, 1980) we do not "smear" the fractures out over a thickness of .2 - 1 m, but actually model them as very small volume elements with no rock matrix present (ϕ = 100%). While this slows computation down by several orders of magnitude, due to throughput limitations in very small grid elements, it is absolutely essential for a realistic modeling of the interaction between matrix and fractures. Our calculations show that, depending upon matrix permeability and liquid water saturation, important variations in thermodynamic conditions near the fracture/

block interface can occur over distances of a few millimeters. Embedding fractures into larger volume elements with plenty of rock would provide an unrealistically large storage of heat which is available for instant equilibration with the fluid in the fracture. This can cause superheated conditions to occur in the fracture, when in fact the liquid water can not be vaporized due to limited conductive heat supply.

The basic radial mesh used in the calculations extends from the effective wellbore radius $r_w' = 20$ m to an outer radius $r_e = 5000$ m, which is large enough so that no boundary effects are felt. Beginning at $r = 20$ m, we use 10 grid blocks with a constant radial increment $\Delta r = 1$ m, and subsequently 30 grid blocks, with Δr increased by a constant factor, such as to obtain an outer boundary at 5000 m. Depending upon the case studied, each grid block is subdivided into 5-9 interacting continua, which form one-dimensional arrays of nested elements. Flow between grid blocks occurs through the fractures only, which are the "outer shells" of the arrays of nested elements. A schematic depiction of the computational mesh is given in Figure 6. The radial grid blocks (solid circles) include the fracture volume with no rock present ($\phi = 100\%$). Radial connections have an inferface area $2\pi rh$, and the radial permeability is the average permeability of the fracture system, as given by eq. (13). Subdivisions of the rock volume enclosed by the fractures are specified as a sequence of increasingly larger fractions of the total volume. Each of the radial grid blocks is connected to a one-dimensional array of nested matrix grid blocks (solid squares), with volumes, interface areas, and distances defined by proper scaling from the geometrical quantities of the basic elementary units as shown in Figure 5. Thus, the matrix acts as a "one-way street" for fluid and heat flow, with all flow occurring outward into the fractures as production causes pressures and temperatures to decline in the fractures. It is possible to generalize this scheme and to permit throughflow through the matrix, but we believe that the restriction to one-way flow as shown in Figure 6 is adequate for the present problem. It is to be noted that vertical fluid and heat flow are neglected in our model, except for flow betwen matrix and fractures. This approximation appears justified, because gravity effects and vertical heat flow will tend to compensate each other, so that our chosen initial conditions will be dynamically stable.

We have investigated three cases with a rock matrix permeability of 10^{-15} m^2, 10^{-16} m^2, and 10^{-17} m^2, respectively. These values are believed to be applicable to The Geysers. With smaller matrix permeability, the processes become more and more confined to the vicinity of the fractures, requiring a larger number of nested volume elements with small volume fractions near the fractures. Some experimentation was required to obtain a gridding which would give adequate spatial resolution without excessive computing costs.

6. Discussion

The fractured reservoir calculations were compared with those for a uniform porous medium having the same permeability x thickness product. Calculations for a relatively low initial water saturation of $S_\ell = 50\%$, corresponding to a relative permeability $k_\ell = .009$, showed that superheated conditions are approached rapidly in all cases. Subsequently we investigated the case with $S_\ell = 70\%$, corresponding to $k_\ell = .143$, which we believe more representative of previously unexploited deeper horizons at The Geysers. Results for the change of production enthalpy and temperature with time are given in Figures 7 and 8.

The fluid mass contained in the wellbore can sustain the applied production rate for 780 seconds, so that the responses of the various fractured and porous medium-type reservoirs do not become markedly different until after this time has elapsed. Subsequently, the fractured reservoirs display a more rapid increase in produced enthalpy, while declining more rapidly in temperature. This behavior is a consequence of the small mass reserves in the fractures, which tend to become rapidly depleted, causing liquid saturation to decline and enthalpy to rise. Boiling of water is initially confined to the immediate vicinity of the fractures, causing a more rapid temperature decline. The production-induced pressure drop diffuses rapidly outward in the fracture system, providing for a larger fracture/matrix interface area through which an increasing share of the fluid produced from the fractures can be replenished by leakage from the matrix.

This prevents the fractures from drying up in the cases with $k = 10^{-15}$ m^2, and $k = 10^{-16}$ m^2, and a steam/water mixture continues to be produced. For the low matrix permeability of $k = 10^{-17}$ m^2, however, the fractures are depleted rapidly, giving rise to superheated conditions. Enthalpy and temperature continue to increase slowly after superheated conditions are reached ($t = 1200$ seconds). This is in agreement with the analysis of section 2: for $k = 10^{-17}$ m^2 the effective permeability for water is $k_\ell k = .143 \times 10^{-17}$ $m^2 < k_{lim} = .527 \times 10^{-17}$ m^2, so that the two-phase flow into the fractures occurs with an enthalpy in excess of that of saturated steam, even though liquid water is mobile. For the two cases with larger matrix permeability we have $k_\ell k > k_{lim}$, so that the fractures are not expected to dry up. The case with a large matrix permeability of $k = 10^{-15}$ m^2 shows an interesting behavior at later times, when the produced enthalpy actually drops below that of the uniform porous medium case. This shows that the fractures have an ample supply of fluid from the matrix, but their heat supply is limited. In contrast, in the case with $k = 10^{-17}$ m^2 the fractures are low on fluid but have plenty of heat supply available. It appears that, due to the fractured nature of the reservoir, the low matrix permeability of 10^{-17} m^2 is quite sufficient to sustain the applied realistic production rate.

Unfortunately, we have not been able to run this latter case further out in time, due to excessive computing costs. Production causes the superheated steam zone to expand rapidly in the fractures (and slowly into the matrix), giving rise to repeated phase transitions with highly transient flows at the steam/two-phase interface. These transients occur in elements with very small volumes, which severely limits attainable throughputs and time steps.

7. Conclusions

The following conclusions may be drawn from this study:

1. For flowing steam/water mixtures there exists a one-to-one correspondence between pressure and temperature gradients, which increases the effective flowing enthalpy due to conductive heat transfer.

2. If the effective permeability for liquid flow (absolute permeability x relative permeability) drops below a limiting permeability k_{lim}, steam will be produced even when liquid water is mobile and flowing. k_{lim} depends upon temperature and heat conductivity, and is typically of the order of 5×10^{-18} m^2 (5 microDarcies).

3. Gravitational drainage of water from a rock matrix with small vertical permeability can be compensated by upward flow of steam in fractures, resulting in very small net vertical mass flux and large convective heat flux. Estimates for The Geysers show that large water saturations in the matrix are compatible with the observed heat flux and with nearly vapor-static pressure gradients for reasonable values of fracture and matrix permeability, respectively.

4. Simulation studies demonstrate that, under conditions applicable to The Geysers vapor-dominated reservoir, the matrix-fracture interaction can

provide a mechanism by which superheated steam is produced from a reservoir with a large water content and a mobile liquid phase. This observation suggests that vapor-dominated geothermal reservoirs may contain significantly larger fluid reserves than was believed previously.

5. A multiple interacting continuum method (MINC) has been shown to be a powerful tool for simulating thermal processes in fractured reservoirs. More work needs to be done to improve computational efficiency for problems which involve highly transient flows near propagating phase fronts.

Table 1: Parameters for Numerical Simulation

Formation Properties	
rock grain density	$\rho_R = 2400\ kg/m^3$
rock specific heat	$C_R = 960\ J/kg^oC$
rock heat conductivity	$K = 4\ W/m^oC$
porosity	$\phi = .08$
permeability x thickness	$kh = 13.4 \times 10^{-12}\ m^3$
reservoir thickness	$h = 500\ m$
matrix permeability	$k_1 = 10^{-15}\ m^2,\ 10^{-16}\ m^2,\ 10^{-17}\ m^2$
Fractures	
three orthogonal sets	
width	$\delta = 2 \times 10^{-4}\ m$
spacing	$D = 50\ m$
permeability per fracture	$k_f = \delta^2/12 = 3.3 \times 10^{-9}\ m^2$
equivalent continuum permeability	$k_2 \approx 2\ k_f\ \delta/D = 26.8 \times 10^{-15}\ m^2$
equivalent continuuum porosity	$\phi_2 \approx 3\delta/D = 1.2 \times 10^{-5}$
Initial Conditions	
temperature	$T = 243\ ^oC$
liquid saturation	$S_\ell = 50\%,\ 70\%$
Production	
wellbore radius	$r_w = .112\ m$
skin	$s = -5.18$
effective wellbore radius	$r_w' = r_w e^{-s} = 20.0\ m$
wellbore storage volume	$V_w = 27.24\ m^3$
production rate	$Q = 20\ kg/s$

Notation

C_R	rock heat capacity, J/kg°C
D	fracture spacing, m
$\underset{\sim}{e}_r$	horizontal vector of unit length
$\underset{\sim}{e}_z$	vertical vector of unit length (pointing upward)
$\underset{\sim}{F}_\ell$	liquid flux, $kg/m^2 \cdot s$
$\underset{\sim}{F}_v$	vapor flux, $kg/m^2 \cdot s$
$\underset{\sim}{F}_\alpha$	flux of phase α, $kg/m^2 \cdot s$
$\underset{\sim}{g}$	gravitational acceleration, m/s^2
h	reservoir thickness, m
h_ℓ	specific enthalpy of liquid, J/kg
h_v	specific enthalpy of vapor, J/kg
K	heat conductivity, W/m· °C
k	permeability, m^2
k_f	fracture permeability, m^2
k_ℓ	relative permeability for liquid, dimensionless
k_{1im}	limiting effective permeability, m^2
k_v	relative permeability for vapor, dimensionless
k_z	vertical permeability, m^2
k_α	relative permeability for phase α, dimensionless
k_1	average permeability of matrix, m^2
k_2	average permeability of fractures, m^2
P	pressure, N/m^2
Q	production rate, kg/s
$\underset{\sim}{q}$	heat flux, W/m^2

r radial coordinate, m

r_e outer radius of reservoir, m

r_w wellbore radius, m

r'_w effective wellbore radius, m

s skin, dimensionless

S_ℓ liquid saturation, dimensionless

$S_{\ell r}$ residual immobile liquid saturation, dimensionless

S_{sr} residual immobile vapor saturation, dimensionless

S^* parameter in relative permeability functions, dimensionless

T temperature, ^oC

t time, s

V_w wellbore storage volume, m^3

v_ℓ specific volume of liquid, m^3/kg

v_v specific volume of vapor, m^3/kg

z vertical coordinate, m

α phase ($\alpha = \ell$: liquid, $\alpha = v$: vapor)

γ vertical pressure gradient in excess of vapor-static, in units of vapor-static gradient

δ fracture width, m

μ_ℓ liquid viscosity, $N \cdot s/m^2$

μ_v vapor viscosity, $N \cdot s/m^2$

μ_α viscosity of phase α, $N \cdot s/m^2$

ν_g gravitational correction to fraction of liquid flux vaporized, dimensionless

ν_o fraction of liquid flux vaporized, dimensionless

ρ_ℓ liquid density, kg/m^3

ρ_R rock density, kg/m^3

ρ_v vapor density, kg/m^3

ρ_α density of phase α, kg/m^3

ϕ porosity, dimensionless

ϕ_2 equivalent continuum porosity of fractures, dimensionless

Acknowledgment

We thank G.S. Bodvarsson and O. Weres for a critical review of the manuscript. This work was supported by the Assistant Secretary for Conservation and Renewable Energy, Office of Renewable Technology, Division of Geothermal and Hydropower Technologies, of the U.S. Department of Energy under Contract No. W-7405-ENG-48.

References

Arihara, N., 1974: "A Study of Non-Isothermal Single and Two-Phase Flow through Consolidated Sandstones," Ph.D. dissertation, SGP-TR-2, Stanford University, November 1974.

Celati, R., Marconcini, R., Neri, G., Pruess, K., Schroeder, R.C., and Witherspoon, P.A., 1979: "Task 3/7 — Modeling Vapor Dominated Geothermal Reservoirs," unpublished report, Pisa, Italy, December 1979.

Counsil, J.R., and Ramey, H.J., Jr., 1979: "Drainage Relative Permeabilities Obtained from Steam-Water Boiling Flow and External Gas Drive Experiments," Geothermal Resources Council, Transactions, vol. 3, p. 141-143, September 1979.

d'Amore, F., and Truesdell, A.H., 1979: "Models for Steam Chemistry at Larderello and The Geysers," Proc. Fifth Workshop Geothermal Reservoir Engineering, Stanford University, December 1979.

Dykstra, H., 1981: "Reservoir Assessment of The Geysers Field - Reservoir Engineering," unpublished report to the California Division of Oil and Gas, Sacramento, California, April 1981.

Eastman, G.Y., 1968: "The Heat Pipe," Scientific American, vol. 218, p. 38-46, May 1968.

Faust, C.R., and Mercer, J.W., 1979: "Geothermal Reservoir Simulation - 2. Numerical Solution Techniques for Liquid- and Vapor-Dominated Hydrothermal Systems," Water Res. Research, vol. 15, no. 1, p. 31-46, February 1979.

James, R., 1968: "Wairakei and Larderello: Geothermal Power Systems Compared," New Zealand J. of Science 11, 706-719, December 1968.

Koenig, J.B., and Sanyal, S.K., 1981: "Availability of Geothermal Steam on Leases CA-5636 and CA-5637, The Geysers, Lake and Sonoma Counties, California," unpublished report, Berkeley, California, February 1981.

Lipman, S.C., Strobel, C.J., and Gulati, M.S., 1977: "Reservoir Performance of The Geysers Field, "Proceedings of the ENEL-ERDA Workshop, Larderello, Italy, p. 233-255, September 1977.

Marconcini, R., McEdwards, D., Neri, G., Ruffilli, C., Schroeder, R., Weres, O., and Witherspoon, P., 1977: "Modeling Vapor-Dominated Geothermal Reservoirs," Proceedings ENEL-ERDA Workshop, Larderello, Italy, September 1977.

Moench, A.F., 1978: "The Effect of Thermal Conduction upon Pressure Drawdown and Buildup in Fissured, Vapor-Dominated Geothermal Reservoirs," Proc. Fourth Workshop Geothermal Reservoir Engineering, Stanford University, December 1978.

Moench, A.F., and Neri, G., 1979: "Analysis of Gabbro 1 - Steam Pressure Buildup Test," Proc. Fifth Workshop Geothermal Reservoir Engineering, Stanford University, December 1979.

Moench, A.F., and Denlinger, R., 1980: "Fissure-Block Model for Transient Pressure Analysis in Geothermal Steam Reservoirs," Proc. Sixth Workshop Geothermal Reservoir Engineering, Stanford University, December 1980.

Narasimhan, T.N., 1980: "Multidimensional Numerical Simulation of Fluid Flow in Fractured Porous Media," to be published in Water Res. Research.

Nathenson, M., 1975: "Some Reservoir Engineering Calculations for the Vapor-Dominated System at Larderello, Italy," U.S. Geological Survey, Open File Report 75-142, April 1975.

Pruess, K., and Schroeder, R.C., 1980: "SHAFT79 User's Manual," Lawrence Berkeley Laboratory Report LBL-10861, Berkeley, California, March 1980.

Pruess, K., and Truesdell, A.H., 1980: "A Numerical Simulation of the Natural Evolution of Vapor-Dominated Hydrothermal Systems," Proc. Sixth Workshop Geothermal Reservoir Engineering, Stanford University, December 1980.

Pruess, K., and Narasimhan, T.N., 1981: "A Practical Method for Modeling Heat and Fluid Flow in Fractured Porous Media," in preparation.

Ramey, H.J., Jr., 1968: "A Reservoir Engineering Study of The Geysers Geothermal Field," Reich and Reich, Petitioners, vs. Commissioner of Internal Revenue, 1969 Tax Court of the United States, 52 T.C. No. 74, 1970.

Truesdell, A.H., and White, D.E., 1973: "Production of Superheated Steam from Vapor-Dominated Geothermal Reservoirs," Geothermics vol. 2, no. 3-4, 154-173, September-December 1973.

Warren, J.E., and Root, P.J., 1963: "The Behavior of Naturally Fractured Reservoirs," Soc. of Petroleum Eng. J., p. 245-255, September 1963.

Weres, O., Tsao, K., and Wood, B., 1977: "Resource, Technology and Environment at The Geysers," Lawrence Berkeley Laboratory Report LBL-5231, Berkeley, California, July 1977.

White, D.E., Muffler, L.J.P., and Truesdell, A.H., 1971: "Vapor-Dominated Geothermal Systems Compared with Hot-Water Systems," Econ. Geol. vol. 66, no. 1, p. 75-97, January-February 1971.

Witherspoon, P.A., Wang, J.S.Y., Iwai, K., and Gale, J.E., 1980: "Validity of Cubic Law for Fluid Flow in a Deformable Rock Fracture," Water Res. Research, vol. 16, no. 6, p. 1016-1024, December 1980.

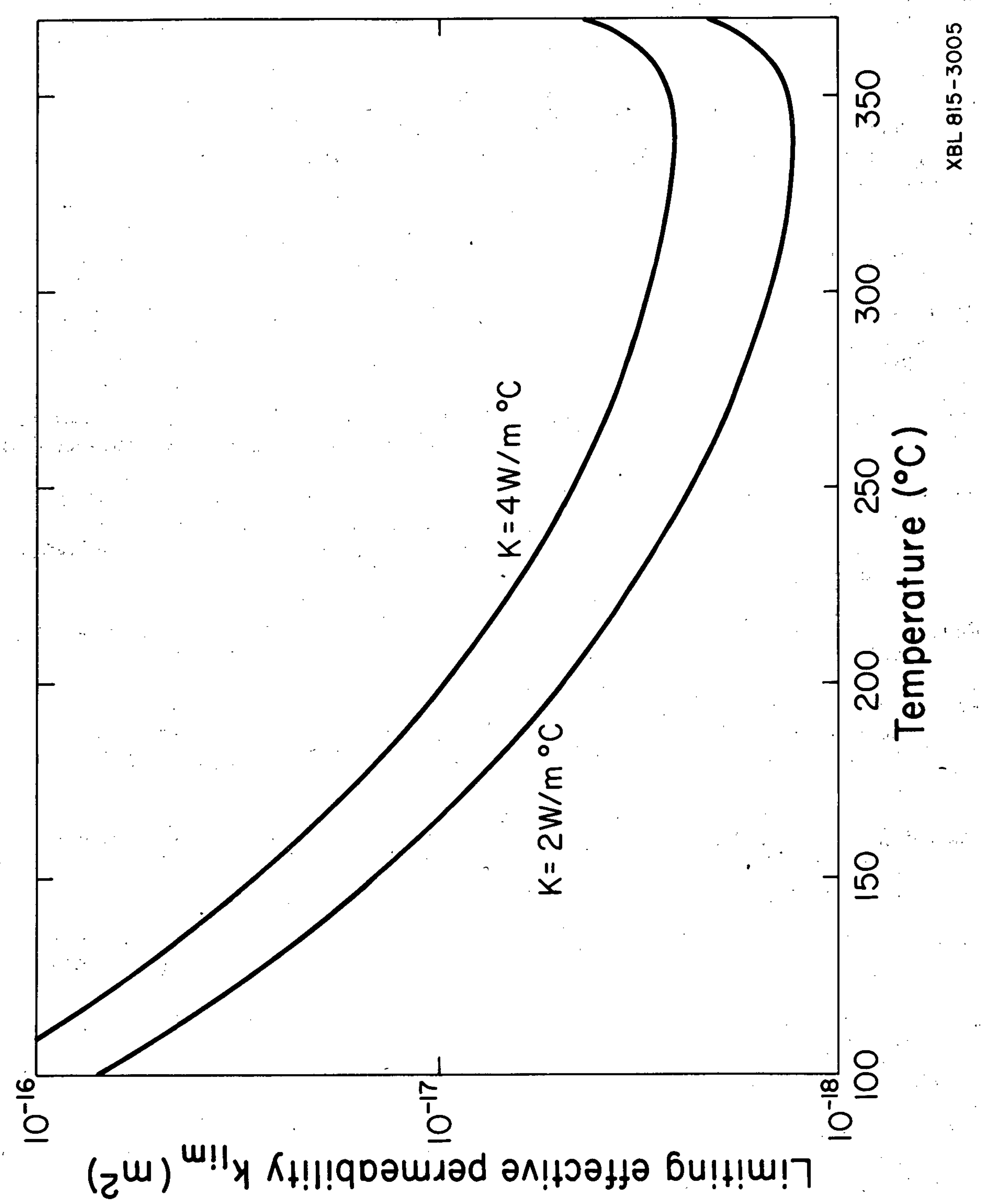

Figure 1: Limiting effective permeability as function of temperature for two different values of heat conductivity (K = 2 W/m °C and K = 4 W/m °C).

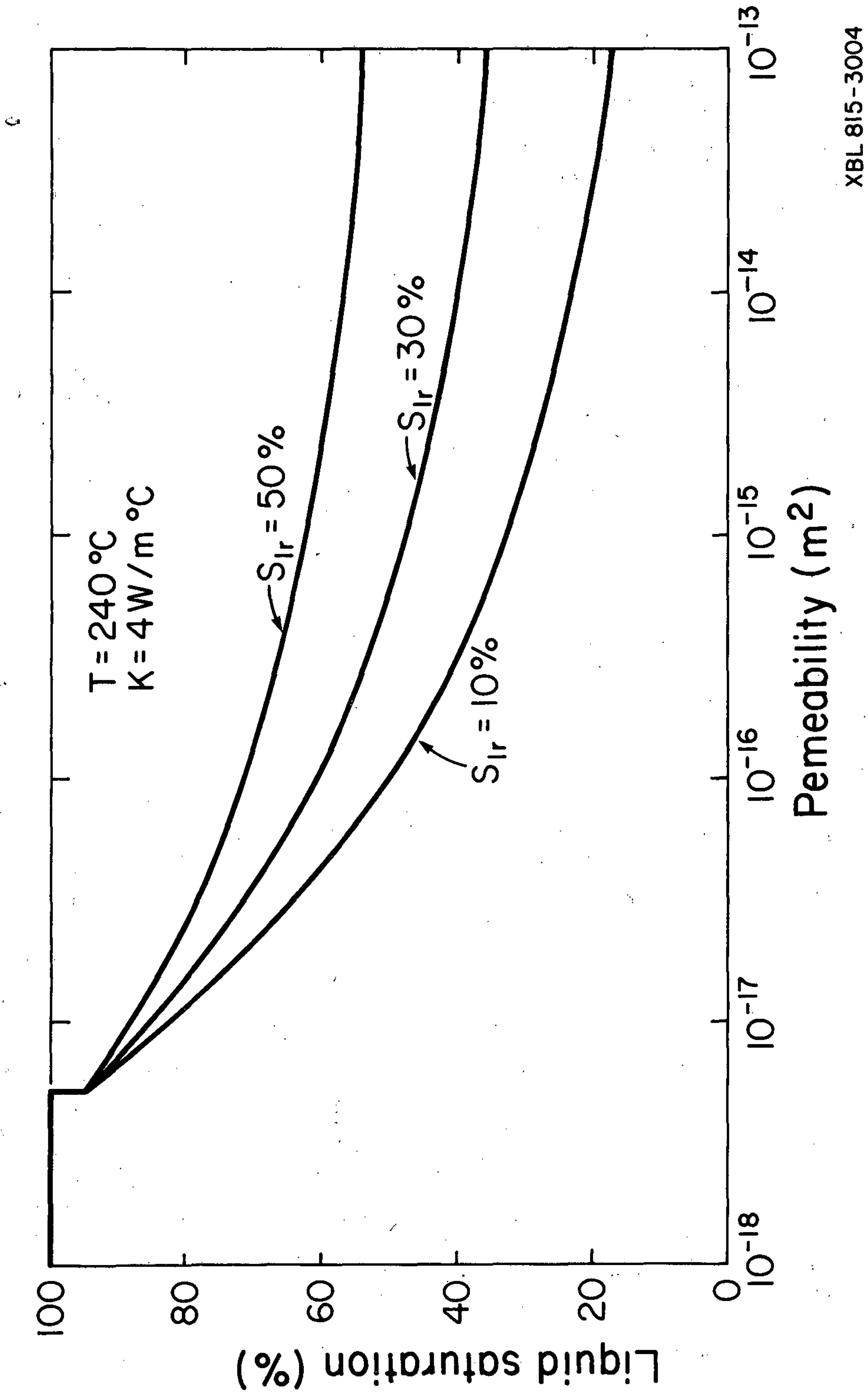

Figure 2: Maximum liquid saturation for complete conductive flashing as function of matrix permeability. The three curves given correspond to different values for residual immobile liquid saturation.

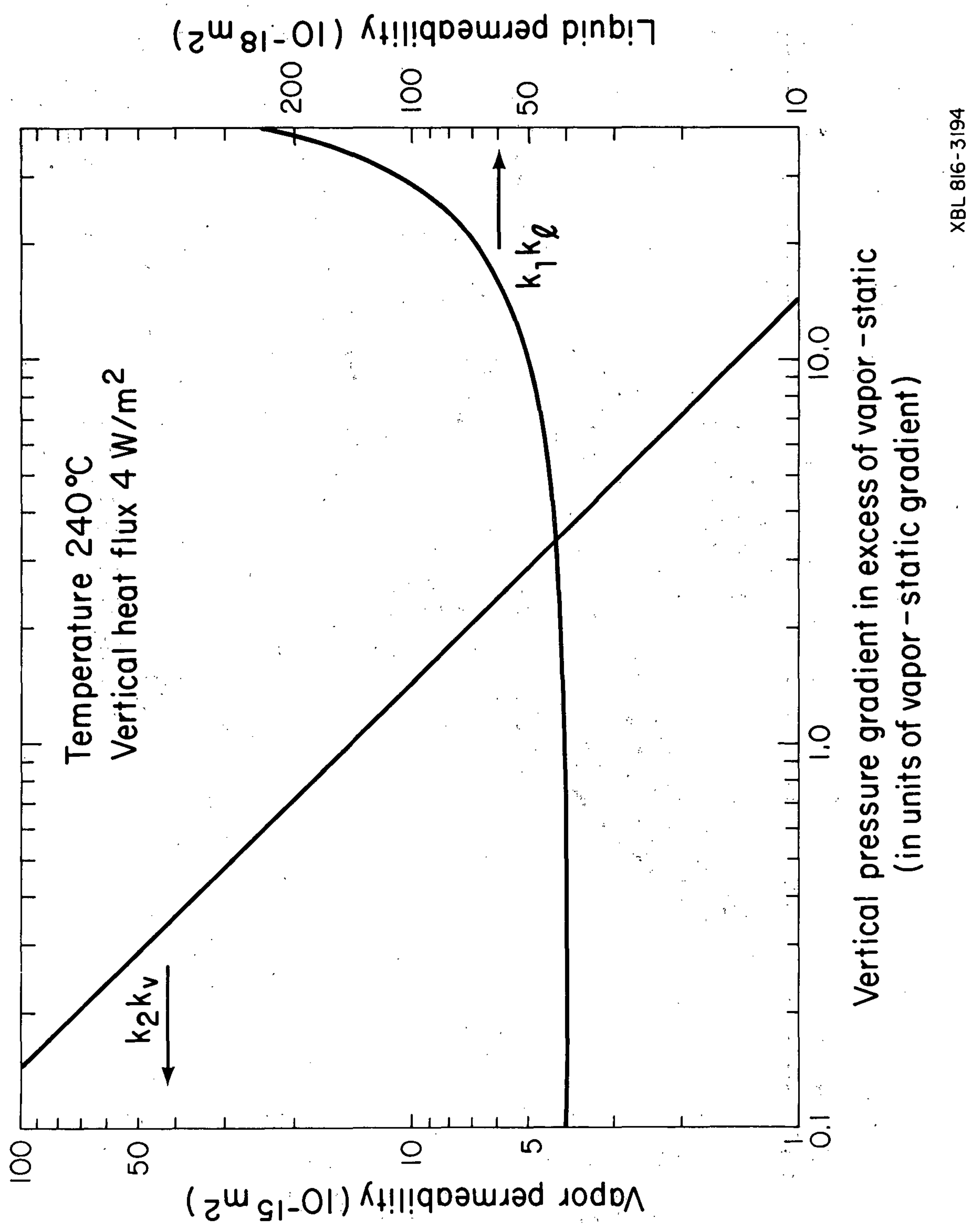

Figure 3: Vertical permeability for vapor and liquid for balanced steam/water counterflow as function of vertical pressure gradient.

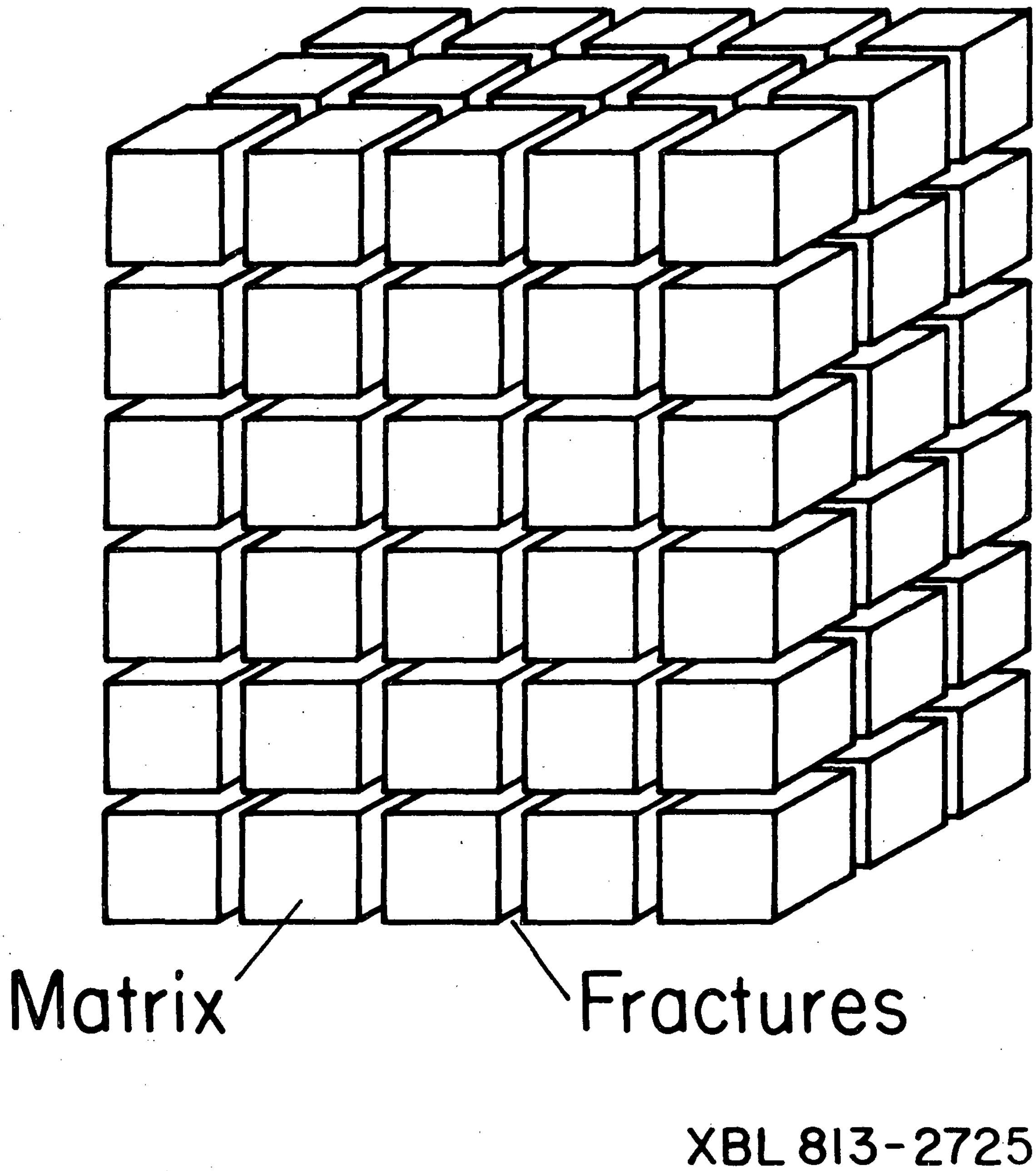

Figure 4: Idealized model of a fractured porous medium.

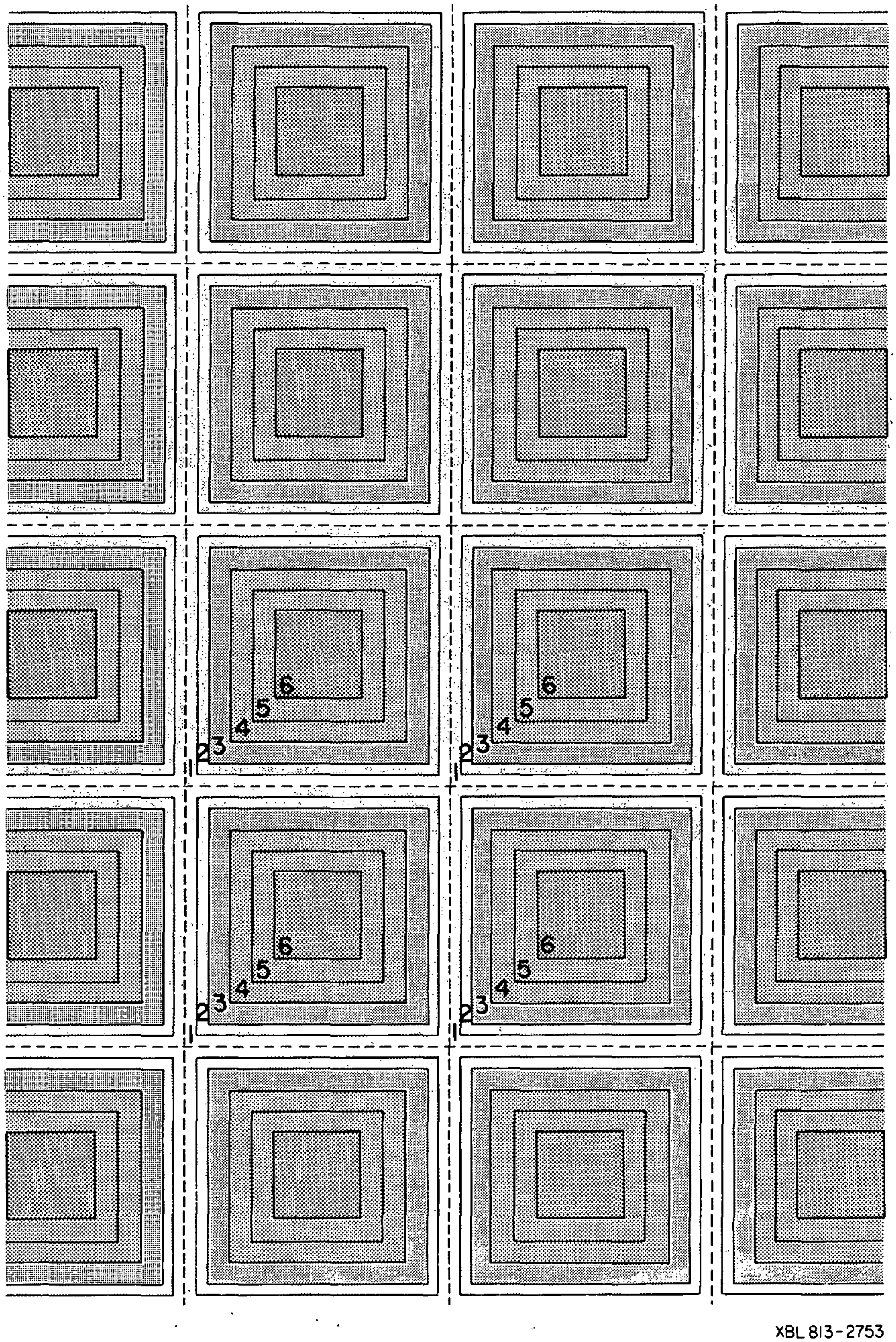

Figure 5: Basic computational mesh for fractured porous media, shown here for simplicity for a two-dimensional case. The fractures enclose matrix blocks of low permeability, which are subdivided into a sequence of nested volume elements.

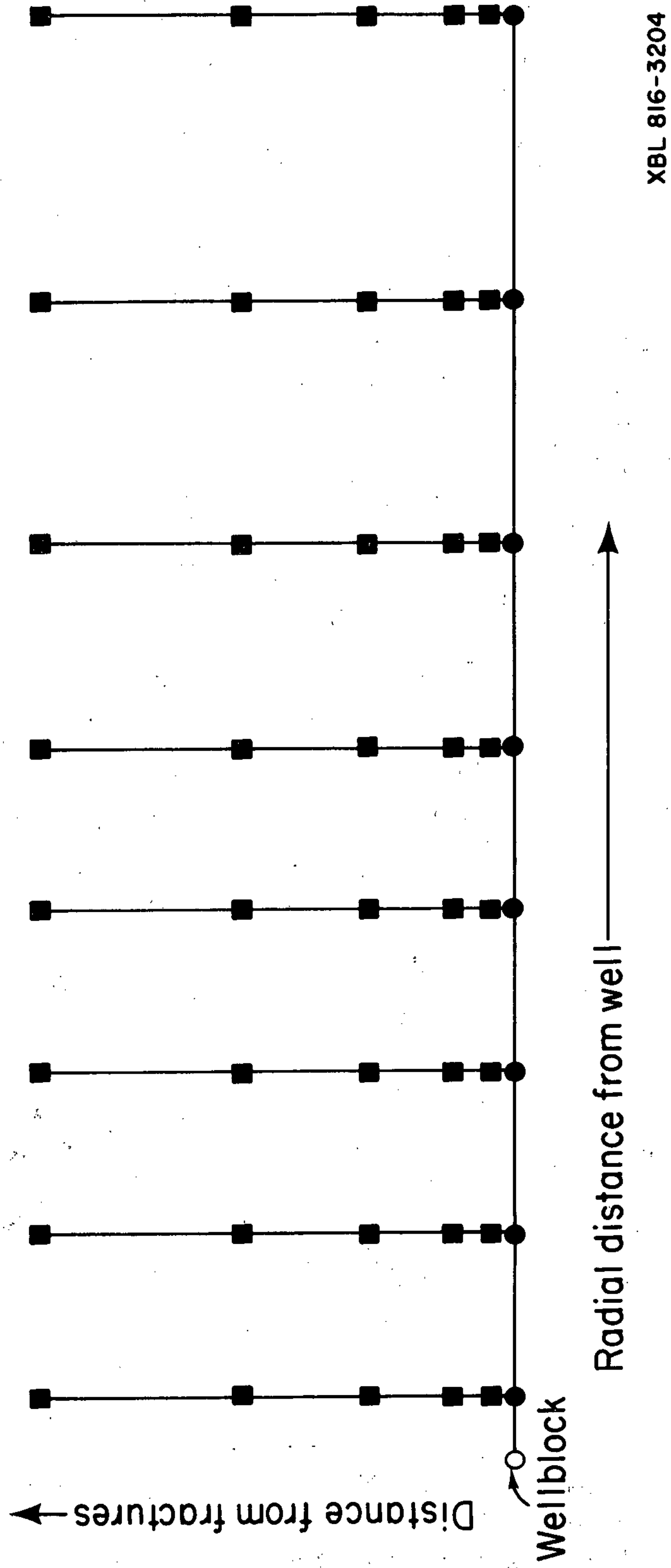

Figure 6: Schematic diagram of the mesh used for computing radial flow in a fractured reservoir.

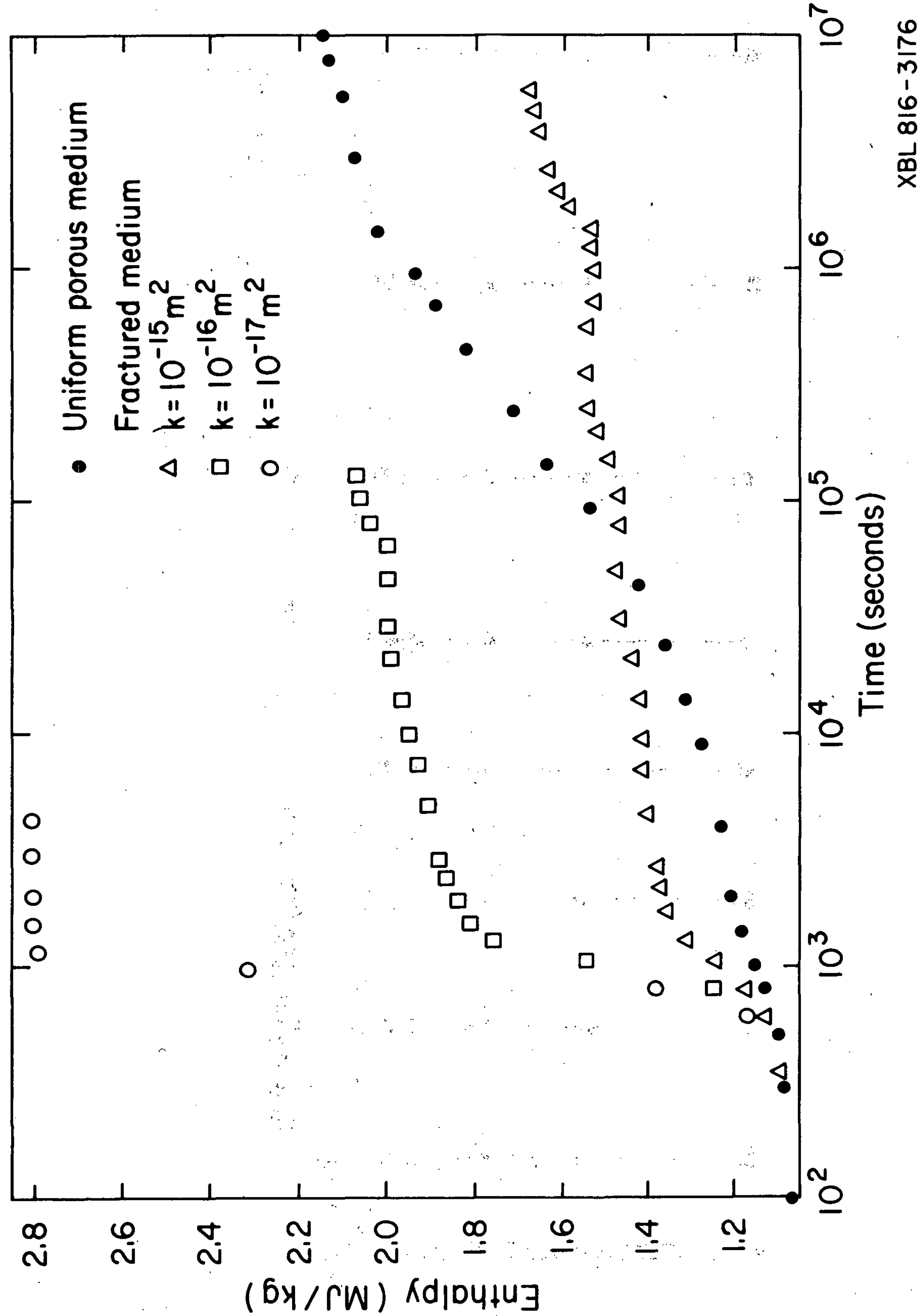

Figure 7: Enthalpy transients for production from two-phase geothermal reservoirs. The behavior of a uniform porous medium is compared with that of fractured reservoirs with different values for matrix permeability.

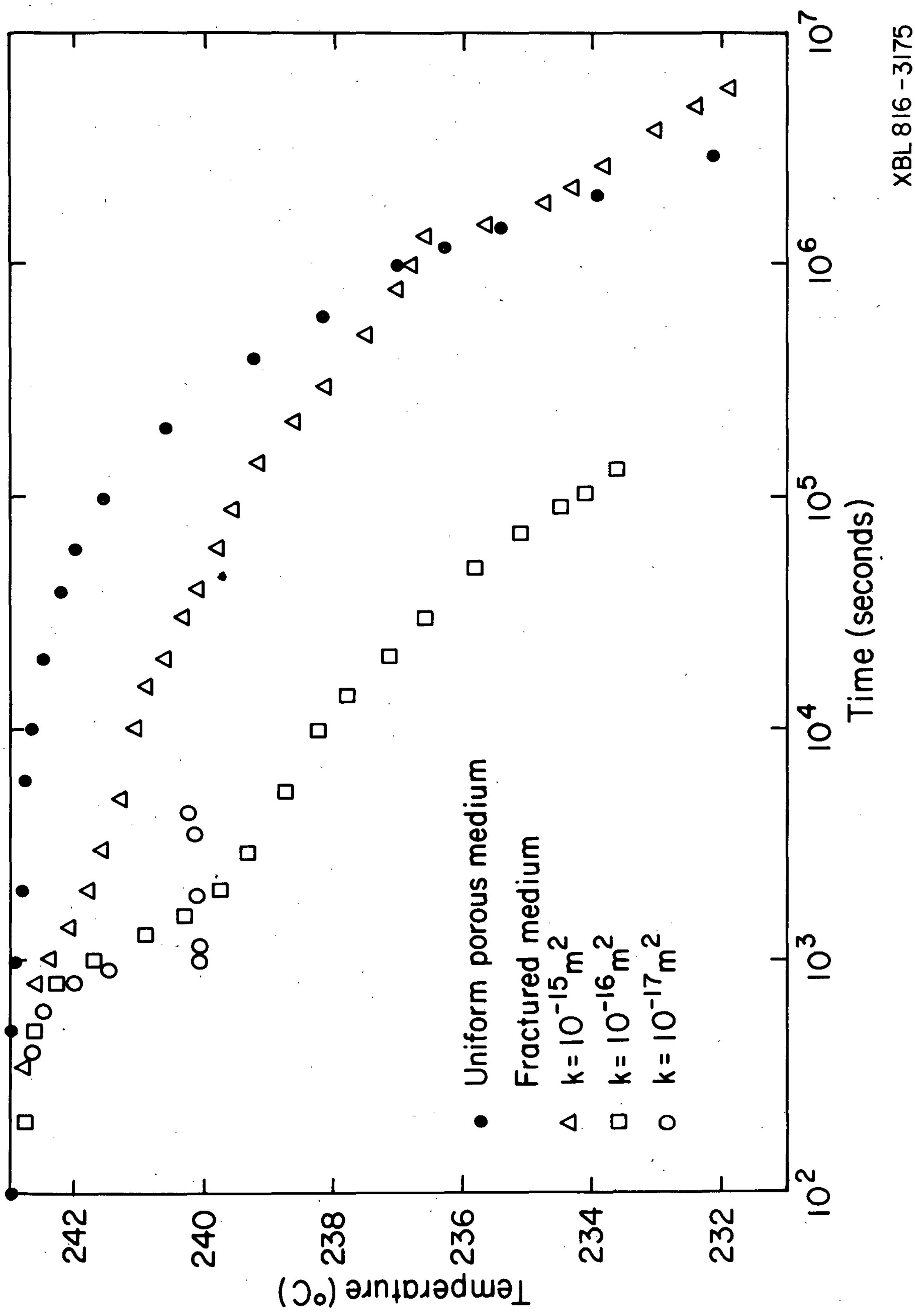

Figure 8: Temperature transients for the same problem as in Figure 6.

TECHNICAL INFORMATION DEPARTMENT
LAWRENCE BERKELEY LABORATORY
UNIVERSITY OF CALIFORNIA
BERKELEY, CALIFORNIA 94720